Electronic Supplementary Material (ESI) for ChemComm.

Supporting Information

Contributions to Activity Enhancement via Fe Incorporation in Ni-(oxy)hydroxide/Borate Catalysts for Near-Neutral pH Oxygen Evolution

Adam M. Smith, Lena Trotochaud, Michaela S. Burke, Shannon W. Boettcher*

Department of Chemistry and Biochemistry and the Materials Science Institute
University of Oregon, Eugene, Oregon 97403

Film Synthesis:

Catalyst films were electrodeposited from 0.4 mM $Ni(NO_3)_2$ solutions buffered to pH = 9.2 with a 0.1 M borate supporting electrolyte on Au/Ti-coated glass electrodes at 0.909 V vs. SCE (not corrected for series resistance) in a three electrode configuration without stirring (Fig. S1 and S2). The electrodes were ~ 1 cm^2 in area. Prior to deposition, solutions were purged with N_2 for ~15 min and subsequently filtered with 0.45 um syringe filter. Borate buffer for deposition was produced from 0.1 M boric acid, respectively (99% purity ACS grade with < 10 ppm Fe for low Fe and Fe-free experiments, or 99.99% purity with < 100 ppm Fe for high Fe experiments) and adjusted to pH 9.2 with KOH (semiconductor grade with < 0.2 ppm Fe for "low Fe and Fe-free" experiments and ACS grade with < 10 ppm Fe for high Fe experiments). All electrochemical experiments were performed with a Biologic SP-200 potentiostat.

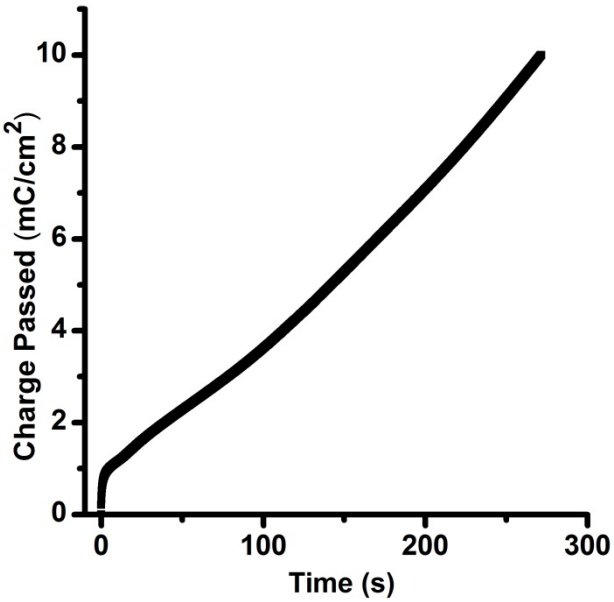

Fig. S1: Representative charge-time trace from Ni-(oxy)hydroxide/borate 10 mC/cm^2 deposition

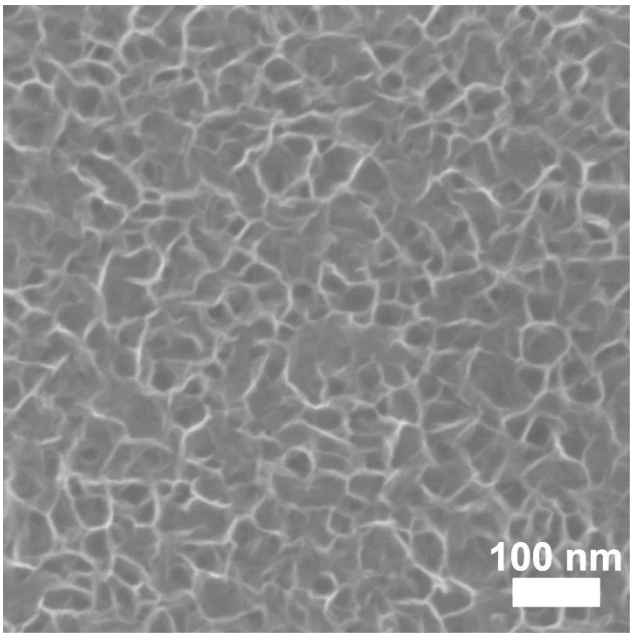

Fig. S2: SEM of as-deposited Ni-(oxy)hydroxide/borate film produced after passing 10 mC/cm^2

Ni-Fe-(oxy)hydroxide)/borate co-deposited samples were similarly synthesized from buffered deposition solutions comprised of 0.36 mM $Ni(NO_3)_2$ and 0.04 mM $FeCl_2$ with 0.1 M borate buffer as supporting electrolyte (Fig. S3 and S4). Ni/borate deposition solutions were purged with N_2 for 15 min before the addition of Fe solutions, after which the combined Ni/Fe solutions were purged for an additional ~10 min and subsequently filtered. Purging was to prevent dissolved O_2 from oxidizing Fe^{2+} to Fe^{3+} which leads to the precipitation of FeOOH in the deposition solution.

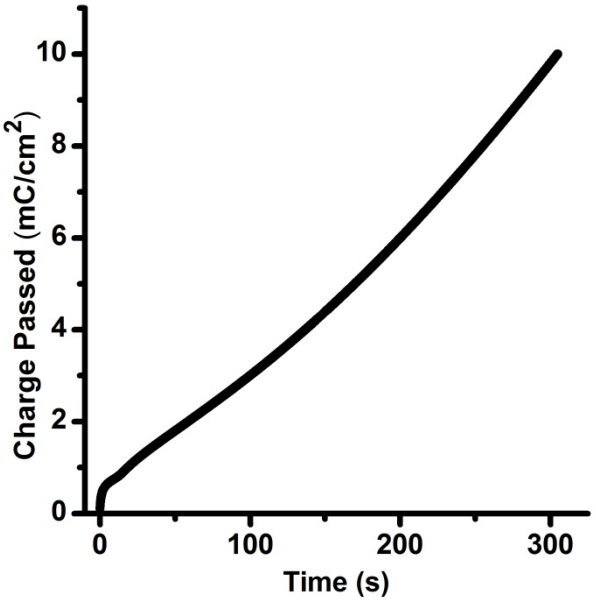

Fig. S3: Representative 9:1 Ni-Fe-(oxy)hydroxide/borate 10 mC/cm^2 deposition

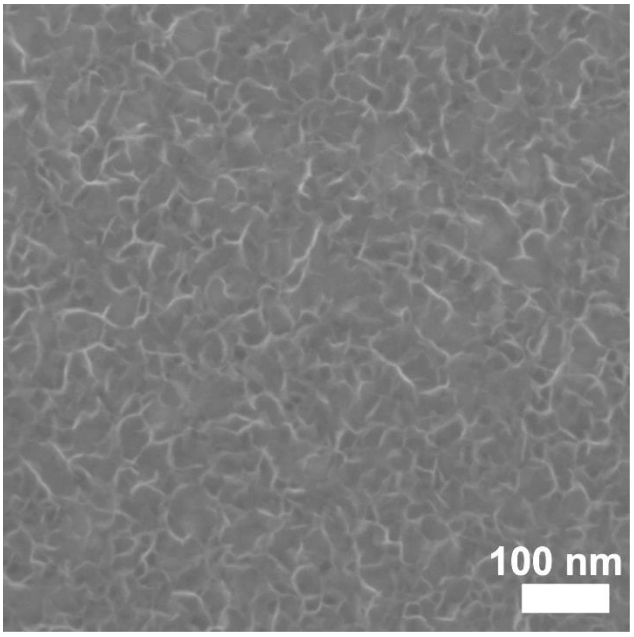

Fig. S4: SEM of as-deposited Ni-Fe-(oxy)hydroxide/borate film produced after passing 10 mC/cm^2

Scanning electron micrographs of catalyst films were taken on a Zeiss Ultra-55 with an in-lens secondary electron detector at an accelerating voltage of 5 keV and a magnification of 50 k. Samples were rinsed and dried at 60 °C prior to imaging.

Film Conditioning:

All catalyst electrodes were removed from the deposition solution, rinsed in high-purity borate buffer and immediately conditioned at 0.856 V vs SCE (not corrected for series resistance) in 0.5 M buffer (99% purity ACS grade with < 10 ppm Fe for low Fe and Fe-free experiments, and 99.99% purity with <100 ppm Fe for high Fe experiments) in a three-electrode electrochemical cell without stirring.

Fe-free electrolyte was produced by purifying 0.5 M borate buffer using $Ni(OH)_2$. Briefly, ~ 2 g $Ni(NO_3)_2$ was dissolved in ~ 4 mL H_2O after which ~20 mL of 1 M high purity KOH was added to precipitate $Ni(OH)_2$. The slurry was then centrifuged and the supernatant decanted. The resulting $Ni(OH)_2$ was then rinsed 3x with high purity KOH (pH = 10.3). Potassium borate electrolyte solution was added to the $Ni(OH)_2$ to remove

Fe and mechanically agitated for 10 min. The electrolyte was subsequently centrifuged, decanted, and stored for later use. Rigorously Fe-free experiments were performed in a Teflon electrochemical cell. Trace Ni species (~ 2.2 μM as estimated below) are dissolved in the purified Fe-free electrolyte solution due to the small solubility of $Ni(OH)_2$ used to absorb Fe.

Film Characterization:

Cyclic voltammograms (CV) were collected starting at 0.756 V vs SCE and scanned between -0.004 V vs SCE to 1.15 V vs SCE at 10 mV/s for three cycles. CV measurements were performed in a three-electrode cell with a Pt counter electrode isolated with a medium porosity glass frit and were not stirred. CV data was corrected for uncompensated series resistance using impedance spectroscopy and calculated at minimum impedance and near-zero phase-angle achieved at high frequency. Typical values for the uncompensated resistance were 10-20 ohms.

Electrochemical experiments (excluding chronopotentiometric Tafel measurements) were performed without stirring. This was done to minimize the influence of Ni-deposition during conditioning in $Ni(OH)_2$ purified electrolyte (Fig. S5) and kept consistent across experiments to provide an accurate comparison of film activity. By not stirring, hysteresis is introduced into CV data (Fig 1); however, this effect is seen across all films and non-stirred experiments show similar behavior as stirred experiments (Fig. S6).

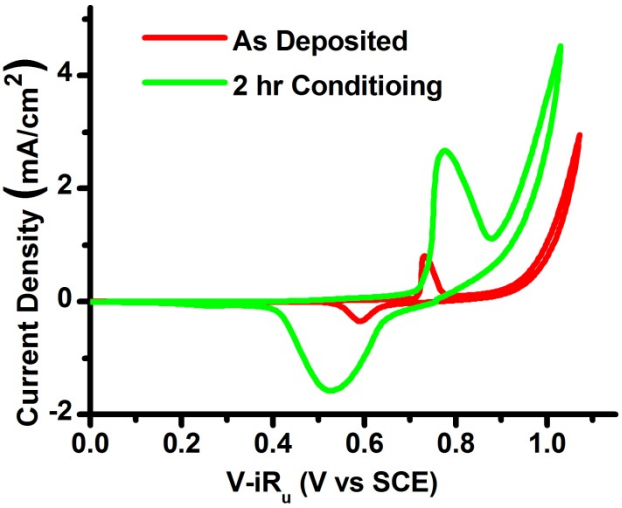

Fig. S5: Cyclic voltammograms of as-deposited and post-conditioning Fe-free films in $Ni(OH)_2$ purified electrolyte. Note the increase in Ni peak areas due to deposition of additional Ni material.

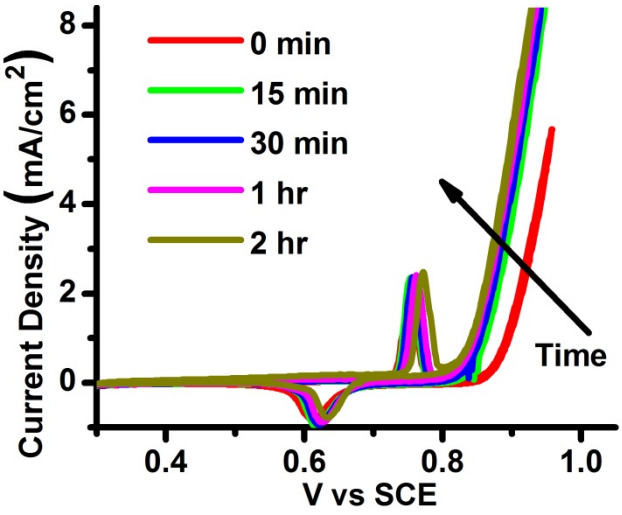

Fig. S6: Cyclic voltammograms of Ni-(oxy)hydroxide/borate film conditioned and measured under stirred conditions.

Turn over frequency (TOF) measurements were taken at intervals after conditioning at 0.856 V vs. SCE. Water oxidation current was measured at 400 mV overpotential (corrected for iR drop) and normalized to the number of active sites via anodic peak integration assuming 1 e^- per Ni site and is consistent with microbalance experiments Fig. S7).

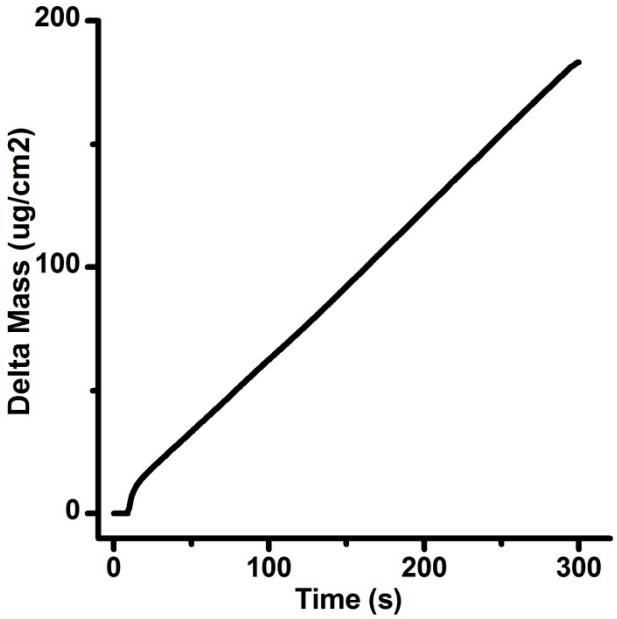

Fig. S7: Quartz-crystal microbalance measurement of change in mass as a function of deposition time

Tafel analysis was performed on films after 2 h of uninterrupted conditioning. Samples were held at various current densities for 10 min before stepping to higher current densities. The measured potential was corrected for uncompensated series resistance and the last 30 data points at each current density were averaged to yield the values in Fig. 2A. Tafel data were normalized to the number of electrochemically active Ni sites. Since Ni is deposited from Fe-free electrolyte solutions when the film is held at anodic potentials, the number of Ni sites as a function of analysis time was approximated from a linear interpolation of the number of Ni sites determined from post-conditioning and post-Tafel CVs. Tafel data normalized to geometric electrode surface area can be found in Fig. S8.

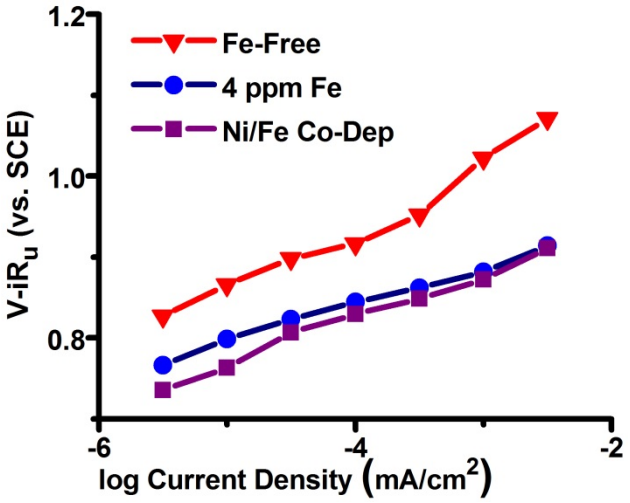

Fig. S8: Tafel data from Fig. 2B normalized to geometric electrode surface area

Ex situ X-ray photoelectron spectroscopy was performed on an Escalab 250 (Thermoscientific) using a non-monochromated Mg source with flood charge neutralization at 200 W, 75 eV pass energy, and a 500 µm spot size. Data analysis was performed using ThermoScientific Avantage v4.75 software. A "Smart" fit was employed to subtract the backgrounds of all spectra and Mg satellite peaks were subtracted. All binding energies were calibrated to the Au4f$_{7/2}$ peak at 84.0 eV.

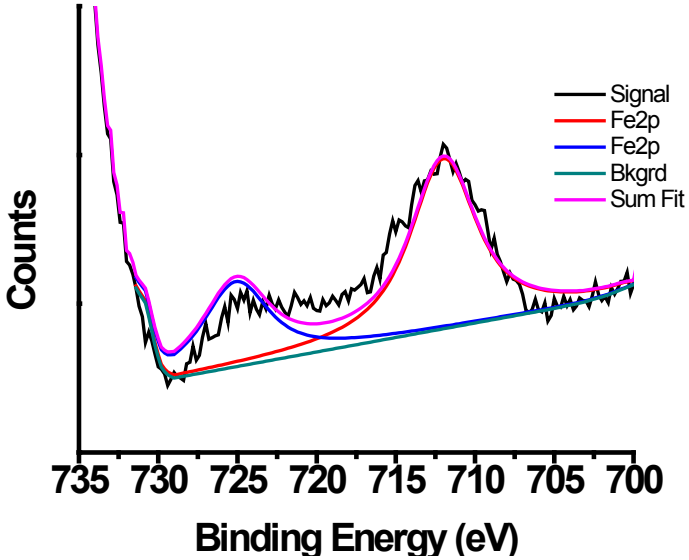

Fig. S9: Representative Fe 2p XPS spectra with peak fitting

Two peaks were used to fit the Fe $2p_{1/2}$ and Fe $2p_{3/2}$ (Fig. S9) peaks and two peaks were used for each Ni environment to fit the Ni $2p_{1/2}$ and Ni $2p_{3/2}$ (Fig. S10) peaks. During peak fitting the following constraints were set; the binding energy of the Fe $2p_{1/2}$ peak was set to 13.6 ± 0.1 eV higher than that of the Fe $2p_{3/2}$, the height of the Fe $2p_{1/2}$ was set to 50% of the height of the Fe $2p_{3/2}$ peak, the FWHM of Fe peaks for a given sample were constrained to be equal, and the Lorentzian-Gaussian % (LG) was constrained to be equal for all Fe peaks. Similarly for the Ni XPS analysis, the binding energy of the Ni $2p_{1/2}$ peak was set to 17.49 ± 0.1 eV higher than that of the Ni$2p_{3/2}$, the height of the Ni $2p_{1/2}$ was set to 50% of the height of the Ni $2p_{3/2}$ peak, the FWHM of Ni peaks for a given sample were constrained to be equal, and the Lorentzian-Gaussian % (LG) was constrained to be equal for all Ni peaks.

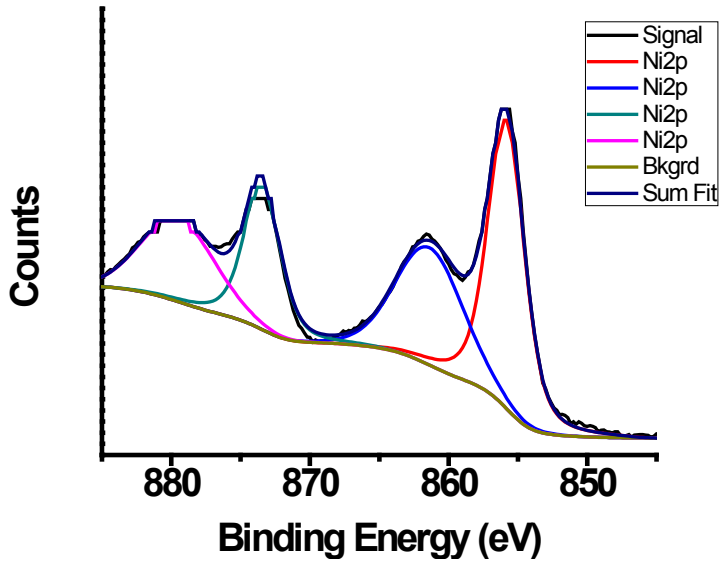

Fig. S10: Representative Ni 2p XPS spectra with peak fitting

Film stability was assessed by conditioning films on quartz-crystal substrates and measuring frequency changes via a microbalance (Fig. S11). Films were found to be stable during anodic conditioning. Films were partially degraded at cathodic potentials during voltammetry and partially re-deposited when held at anodic potentials. We estimate the equilibrium concentration of Ni^{2+} species to be ~2.2 μM at pH 9.2 from a K_{sp}

value of 5.48×10^{-16} for $Ni(OH)_2$, which accounts for the film dissolution observed after voltammetric cycling to potentials where Ni^{2+} is prevalent.

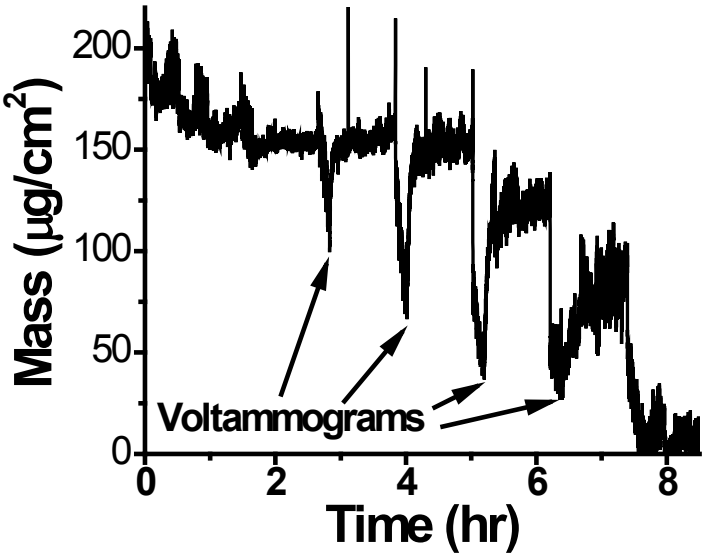

Fig. S11: Quartz-crystal microbalance measurement of change in mass as a function of time conditioned at 0.856 V vs. SCE. Arrows indicate putative film degradation and subsequent partial re-deposition during voltammetric characterization.